7th International Conference on Modelling and Simulation in Nuclear Science and Engineering (7ICMSNSE)
Ottawa Marriott Hotel, Ottawa, Ontario, Canada, October 18-21, 2015

7ICMSNSE-074

MCNP Simulation of the Canadian Super-Critical Water Reactor's Liquid Injection Shutdown System

D. Watts[1]
[1] Canadian Nuclear Laboratories, Chalk River, Ontario, Canada
david.watts@cnl.ca

Abstract

The Canadian Super-Critical Water Reactor (SCWR) uses a vertical pressure-tube concept, with D_2O moderator, super-critical H_2O coolant and thorium-based fuel. To further recent MCNP modelings of the SCWR core, it was necessary to simulate a Liquid Injection Shutdown System (LISS), which involves reactivity reduction by liquid neutron poison injection. By utilizing previous studies on similar reactor concepts, a LISS has been modeled in MCNP for the SCWR, demonstrating sufficient and timely reactivity reduction. In particular, the model propagates physically realistic neutron poison jets over multiple time steps, thereby simulating a realistic LISS in MCNP.

Keywords: Reactor and Radiation Physics, Computer Codes and Modeling, Monte Carlo Methods and Applications, Advanced Reactors & Advanced Fuel Cycles.

1. Introduction

The Canadian Super-Critical Water Reactor (SCWR) is a Gen-IV[1], vertical pressure-tube–based reactor concept, with D_2O moderator, super-critical H_2O coolant and fissile-enriched thorium fuel [2]. The use of super-critical water coolant would significantly increase the thermal efficiency, and hence, net power relative to more conventional reactors, while the use of thorium fuel would greatly increase the inventory of possible fuel.

To further recent CNL[2] studies involving MCNP[3] modelings of the Canadian SCWR (see Figure 1-1), it was necessary to simulate reactivity devices for the SCWR, including emergency Shut-Down Systems (SDSs). Because such systems involve the penetration of the core by neutron-absorbing materials, this is best achieved with a 3-D code such as MCNP [3].

The most difficult SDS to model without a 3-D code is the Liquid Injection Shut-down System (LISS), designated as SDS2[4], which involves reactivity reduction by liquid neutron poison injection. By utilizing previous studies on similar reactor concepts, a LISS has been modeled here in MCNP for the SCWR, demonstrating a sufficient and timely reduction in reactivity. Of particular note, the model propagates physically realistic neutron poison jets over multiple time steps, thereby simulating a realistic LISS in MCNP for the SCWR.

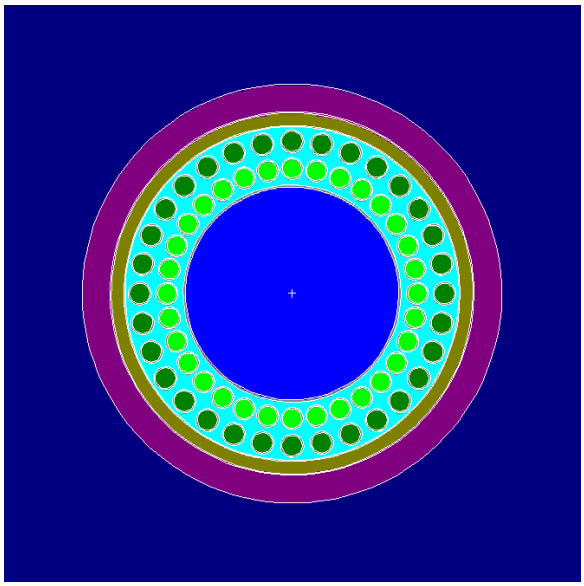

Figure 1-1 Cross-Sectional View of the 64-Element Canadian SCWR Fuel Bundle Concept; High Efficiency Re-entrant Channel (HERC) [1]

1 Gen-IV: Generation 4 [1].
2 CNL: Canadian Nuclear Labs (formerly AECL; Atomic Energy of Canada, Ltd.).
3 'Monte Carlo N-Particle' [3].
4 To distinguish it from SDS1, neutron absorber rod insertions.

2. Models

The Canadian SCWR concept shares with the ACR[5] design the use of D_2O-moderated, H_2O-cooled, pressure-tubed fuel channels [4]. In particular, the D_2O moderator is unpressurized, which allows for the insertion of negative reactivity in the form of Cd absorber rods and Gd-poisoned moderator as means of emergency reactor shutdowns [2]. There are, thus, two Shut-Down Systems (SDSs) being contemplated for the SCWR, paralleling those for the ACR;

SDS1: Shut-Off Rods (SORs) SDS2: Liquid Injection Shut-down System (LISS)

As such, it is possible to use previous investigations into the SDSs modeled for the ACR as starting points for similar models for the SCWR [4]. This paper examines the SDS2 LISS modeled for the ACR as described in reference [4], and uses it as a basis for modeling a similar LISS for the SCWR. That report [4] compares the mathematical model ALITRIG[6] against 'Computational Fluid Dynamics' (CFD[7]) for simulating Gd poison injection into the ACR core.

2.1 ALITRIG-Modified CFD Nozzle-Streams

ALITRIG is a semi-empirical model developed in the 1990s describing poison jet growth into an unpressurized D_2O core based on prototype experiments done in the 1970s at SPEL[8] [4]. Adapted for the ACR, ALITRIG describes the 1-D length (L) of a poison jet over time (t) as a nonlinear function of initiating jet speed (v_0), jet hole diameter (d) & spacing (s), and channel pitch (p) & radius (r) [5]:

$$L = K[v_0 d]^{½} t^{N_0}$$

where expressions for K, N_0 & C_T can be given by [5]:

$$K = K_\infty f_1\{C_T(½p–r)/r\} f_2\{s/d\} \qquad N_0 = ½ f_3\{s/d\} f_4\{(s/d)(½p–r)/r\} \qquad C_T = C v_0^{\,A}$$

and where f_1, f_2, f_3 & f_4 are generalized exponential functions and K_∞, C & A are constants [5].

To simplify application to the SCWR, parameters such as initiating jet speed and jet hole diameter & spacing can be assumed to be the same as in the ACR. However, channel pitch & radius are (as currently conceptualized for the SCWR) different. Also, ALITRIG does not compute the 3-D distribution of poison into the core over time; just the poison jet length [4].

CFD does produce 3-D contoured distributions of [Gd] into the core over time (referred to here as ***isosyncs***[9]; see Figure 2-1) [4], and so would be a preferred modeling approach over ALITRIG. However, CFD modeling results are only available for the ACR-1000 core, and not the SCWR. But while CFD is better at giving *specific* estimations for poison distributions, ALITRIG uses an actual *algorithm* to compute jet-length, dependent on parameters such as channel pitch & radius.

---

5 ACR: Advanced Candu Reactor; trademark of AECL.
6 ALITRIG: Analysis Liquid Injection Test RIG.
7 Using the commercial software ANSYS-CFX 10.0 [4].
8 SPEL: (then) Sheridan Park Engineering Lab (now CANDU Energy Inc.).
9 'isosync': from iso-*synkentrosi;* Greek for constant-*concentration* [6].

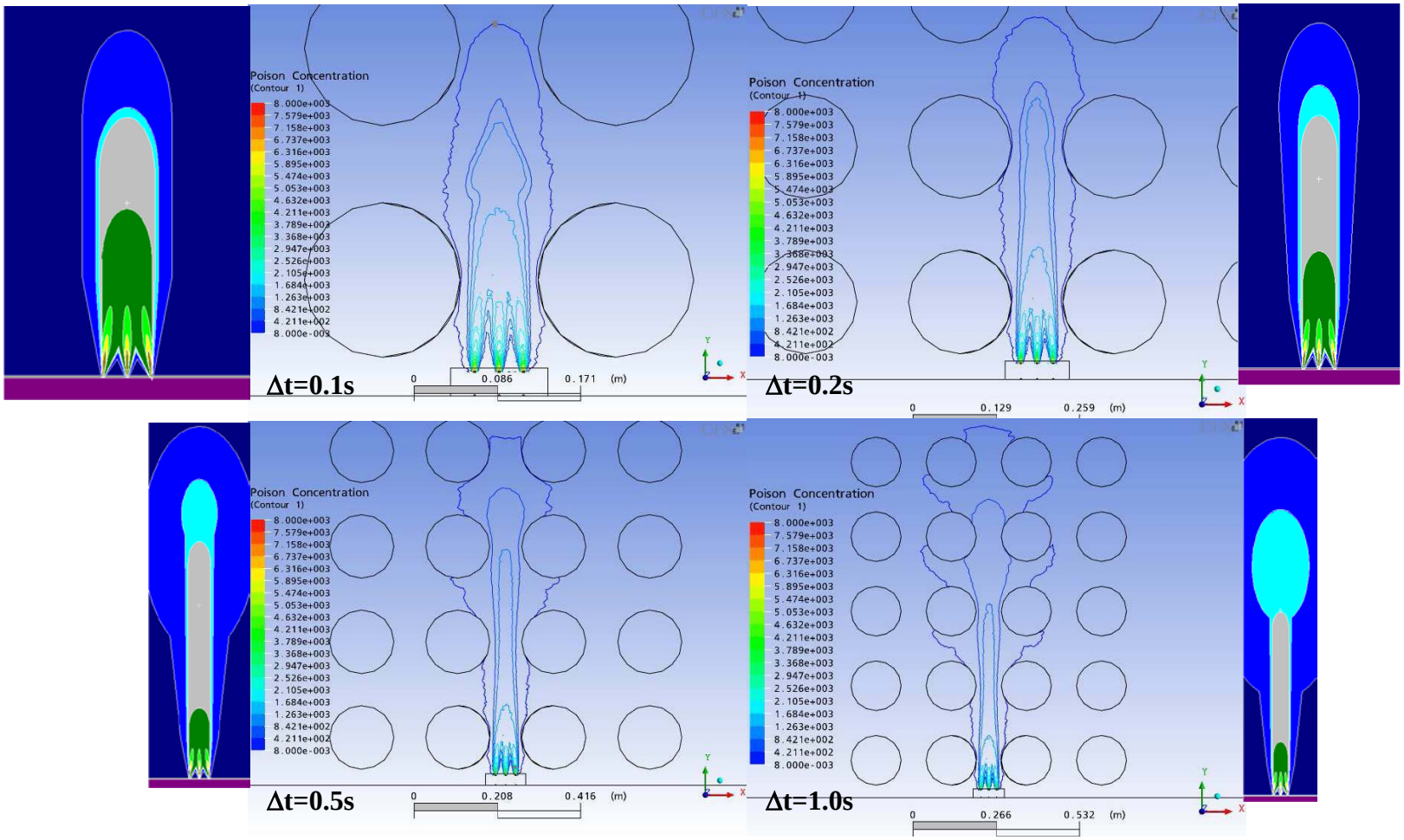

Figure 2-1 CFD [4] & MCNP [Gd] Isosyncs in Unpressurized D_2O over Time

Here, a combined[10] approach is used in which the CFD poison distributions are scaled to the SCWR channel pitch & radius according to the ALITRIG formulation. From the above ALITRIG formulation, one can deduce relative changes in poison jet-length due to changes in channel pitch ($\partial L/\partial p$) or radius ($\partial L/\partial r$), yielding an overall jet-length adjustment of:

$$L' = L + \Delta L \quad \leftrightarrow \quad \Delta L = (\partial L/\partial p)\delta p + (\partial L/\partial r)\delta r$$

where δp & δr are the differences between ACR & SCWR channel pitches & radii, respectively.

These adjustments are applied to each isosync surface individually. That is, the jet-length of each major isosync surface shown in Figure 2-1 can be adjusted according to the ΔL adjustments from ALITRIG, to ensure the relative distribution of poison within each jet-stream remains the same. Figure 2-2 then shows these ALITRIG-adjusted-CFD isosync jet-lengths (L') plotted over time:

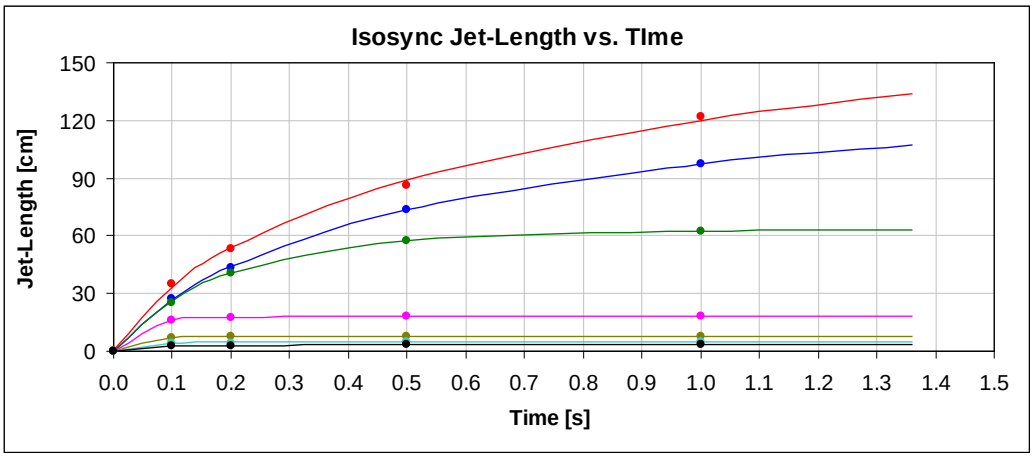

Figure 2-2 ALITRIG-Adjusted-CFD Isosync Jet-Lengths vs. Time

From Figure 2-2, the best-fit curves (found to minimize rms error) for these adjusted jet-lengths (L') are then approximated as generalized inverse power fits: $L' = \alpha_L - \beta_L/(t-\gamma_L)^{\delta_L}$, where 't' is time and 'α_L', 'β_L', 'γ_L' & 'δ_L' are constants. Such a generalized inverse power fit always increases asymptotically, best representing this physical aspect of the isosyncs.

2.2 Modeled Nozzle-Stream Shapes

From Figure 2-1, it can be seen that the nozzle-streams (combined jet-streams) are roughly cylindrical at most times (ignoring the lower tri-conical sections as well as the upper spheroidal caps that 'balloon' at later times). It can also be seen that the nozzle-stream radii across the first narrowing (the restriction of the first row of fuel channels) change very little in each of the 4 time steps. This is due to the lateral constraints placed on the jets by the fuel channels. It will, thus, be assumed, as an approximation, that each isosync midsectional radius is a constant fraction of

[10] Without comparison to actual reactor measurements, it hard to model the speed and shape of the poison injection field in the reactor. But short of redoing an entire CFD analysis applied to the SCWR (which is beyond the scope of this work), a combined ALITRIG-CFD approach would appear to be a reasonable compromise.

channel pitch, unchanging over time. These *nominal* (or *lower*) isosync midsectional radii (R) can be taken from the Δt=0.1s image in Figure 2-1, and are scaled to their *equivalent* radii (R') for the SCWR, using the ratio of p_{SCWR}/p_{ACR} (the ratio of the SCWR pitch to the ACR pitch).

For a given nozzle-stream, the outer 4 isosyncs are each nominally modeled with 3 conical jet-streams merging into a cylindrical midsection, topped off with a spheroidal cap (see Figure 2-1; also Figure 2-3). The bottom 3 sets of isosyncs do not merge, and are each modeled with conical jet-streams topped off with *hemi*spheroidal[11] caps (no cylindrical midsections).

As the nozzle-streams expand, the outer isosyncs tend to balloon; see Figure 2-1's Δt=0.5s & Δt=1.0s. It can be seen that the 1st isosync balloons after it passes the 2nd row of channels, while the 2nd isosync balloons after it passes the 3rd row of channels[12]. To model these balloonings, the midsections must become semi-*conical*; their *upper* midsectional radii[13] (*Я*) can be taken from Figure 2-1 and scaled to their *equivalents* (*Я*') for the SCWR, again using the ratio of p_{SCWR}/p_{ACR}.

The complete simulation of a ballooning isosync (including size & shape) is then outlined in Figure 2-3. The top of the red nozzle-stream's midsection is below the 'ballooning height', and, thus, is still growing and not yet ballooning, while the top of the blue nozzle-stream's midsection has hit the 'ballooning height', and, thus, has stopped growing while its cap is ballooning.

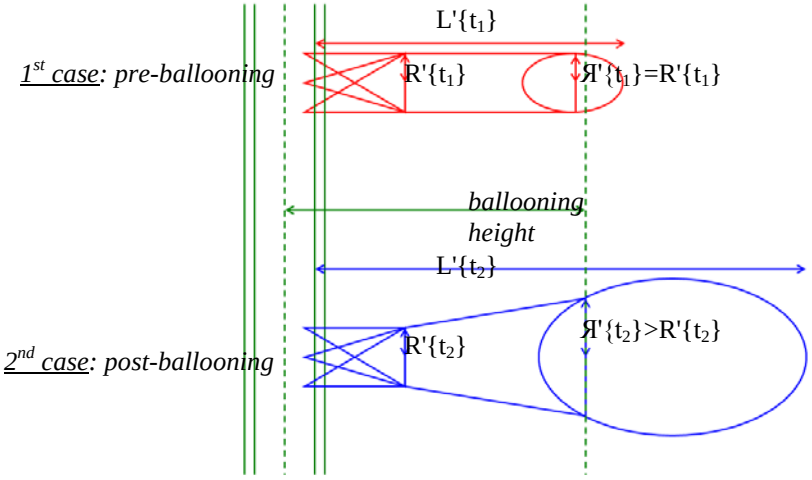

Figure 2-3 Ballooning of Sample Nozzle-Stream

2.3 [Gd] Adjustments

When an isosync intersects fuel channels or when its width expands beyond the constraints imposed by neighboring nozzle-streams (1 channel pitch; see, for example, Δt=0.5s or Δt=1.0s of Figure 2-1) or beyond the end of the hexagonal cell containing an injector (see Figure 2-5), the

---

11 'Hemi'-spheroid as the bottom 3 isosyncs are literally *half* spheroid.

12 As a general rule, it's assumed that the nth isosync will balloon after its upper midsectional height (just below its spheroidal cap) passes the (n+1)th row of channels. In practice, this only affects the 2 outermost isosyncs.

13 *Pre*-ballooning, the *nominal\lower* midsection radius R and the *upper* midsection radius *Я* for a given isosync are presumed equal.

volume of those truncated portions of the isosync is calculated and the poison concentration of the remainder of that isosync is recalculated to preserve total poison mass.

The *gross* volumes of individual isosyncs are found through careful calculation of the total volume contained within each isosync (tilted tri-conical jets, cylindrical\semi-conical mid-section and spheroidal cap), minus any internal overlaps as well as the aforementioned truncations due to lateral or far-end cut-offs and intersections with the fuel channels. The *net* volume for each isosync is then found as the difference between the volume of a given isosync and the volume of the next smaller isosync (except for the 7th isosync, in which the gross volume is also the net volume). From this, one can then adjust the [Gd] of each of the isosyncs such that:

$$f \times \Sigma_{i=1}^{7} [Gd]_i V_i = [Gd]_0 \times A_{node} v_{jet} \times t$$

On the right-hand side, $[Gd]_0$ is the original [Gd] of the injector poison (8000 ppm [7]), A_{node} is the combined area of the node's jets, v_{jet} is the mean poison speed (up to that time; see Sect.2.4), and t is the time that the poison has been flowing through the injector (trip time minus the travel time to that injector node). On the left-hand side, $[Gd]_i$ is the i^{th} isosync's *nominal* [Gd] (see Figure 2-1), while V_i is the i^{th} isosync's net volume. Both sides should yield the volume-integrated amount of Gd injected into the moderator. The factor 'f', found by solving the above equation, is then applied to the values of $[Gd]_i$ (for a given node) to ensure that the total amount of Gd modeled (the left-hand side) matches the total volume of Gd injected (the right-hand side).

2.4 Poison Injector Flow

Given that the flow of poison down the injector is not instantaneous, the time it takes for the poison to reach each of the 19[14] nodes must also be factored in. Figure 2-4 shows a simplified example of poison flow through an injector. The main injector-line has a cross sectional area of A_{inj}, while the individual nodes along the injector each have a combined[15] area of A_{node}. As the poison travels past each node, some of the poison exits via the jets, decreasing the amount of poison flow to the next node, until the last (20th) node. The fluid pressure & speed in the injector up to and including the n^{th} node are listed as P_n & $v_{inj:n}$, respectively, while the jet speed upon exiting a given node is $v_{jet:n}$. The exit pressure, P_x, is the (uniform) pressure of the moderator.

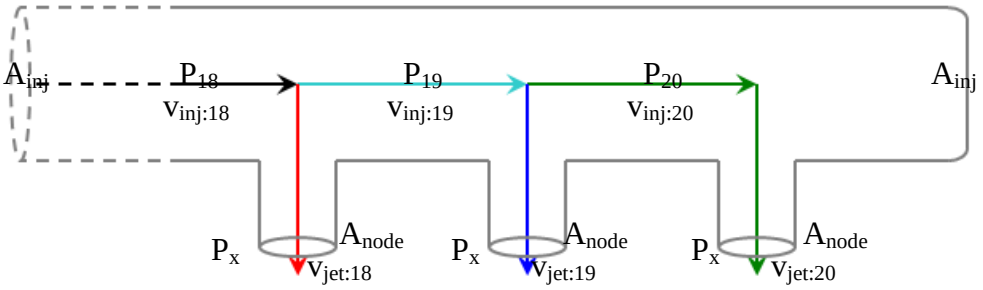

Figure 2-4 Simplified Poison Flow Thru Injector

[14] There are 20 rows of fuel channels, and 19 injector nodes aligned interstitially between them. The nodes are here numbered for the channels that *follow* them, so the 1st & 21st (*outer*) 'nodes' have no nozzles.

[15] The areas of all (3jets/nozzle×6nozzles/node=) 18 jets/node are here combined into a single area A_{node}.

In order to map out the flow of poison both along and from the injectors, the values of $v_{inj:n}$ & $v_{jet:n}$ at each node are required. To determine these values, it will be assumed that the poisoned fluid is both incompressible and ideal (frictionless). This allows use of both the (incompressible) Continuity equation (Av=const) and the (ideal) Bernoulli equation ($P+\frac{1}{2}\rho v^2=const$[16]).

In applying[17] the Bernoulli[18] equation, it can be shown that the jet speeds are all equal (which can then be set to a uniform v_{jet}), while application of the Continuity equation yields for the speed of poisoned fluid along the injector[19]:

$$v_{inj:n}\{t\} = v_{jet}\{t\}[(N-n+1)A_{node}/A_{inj}] \qquad 2 \le n \le N$$

where $v_{inj:n}$ is the injector poison speed at the n^{th} node; 'N' is the maximum node # (here, 20), v_{jet} is the (uniform) jet speed, and A_{node} & A_{inj} are the jet-nodal & injector areas, respectively.

Upon injection, the poison flow is *relatively* constant (~30-25m/s [7]) for ~1 s, after which the flow then falls off sharply to 0 as the pressure tanks deplete. However, although the poison speed stays *relatively* constant for ~1 s, it does show a *slight* fall-off, with a *moderate* deceleration rate, a_{jet}, which can be related to the deceleration of the injector-line poison as: $a_{inj:n} = a_{jet}[(N-n+1)A_{node}/A_{inj}]$. Using basic kinematics, the timing of the leading edge of the injector-line poison as it passes the n^{th} node[20] for the first time can then be given recursively as:

$$t_n = t_{n-1} + (-v_{inj:n}\{t_{n-1}\}+[v_{inj:n}\{t_{n-1}\}^2+2a_{inj:n}\Delta d]^{\frac{1}{2}})/a_{inj:n} \qquad \leftarrow \Delta d = 1 \text{ pitch}$$

with a_{jet}, N, A_{node} & A_{inj} all given. The values of t_n found from this algorithm can then be used to 'delay' the injection of the jet streams at the n^{th} node. This allows a realistic delay effect in the propagation of poison into the core; see Figure 2-5 for the resulting poison injection model.

2.5 Poison Injector Assembly

As shown in the right-hand set of images in Figure 2-5, there are 7 injectors arrayed in a hexagonal lattice (similar to the 8 injector assembly proposed for the ACR-1000 [4]), matching the hexagonal arrangement of nozzle-streams emanating from each node. The hexagonal cells

---

[16] The injectors are assumed horizontal and the 'nozzle heights' are small enough (dh_{nzl}~0 [5]) so that the gravity term in the Bernoulli equation, ρgh, can be ignored. Additionally, this 'ideal' version of the Bernoulli equation assumes no forced pumping (ΣW_{pump}~0) and no frictional (head) losses (ΣH_{loss}~0) [8]. (In fact, there are both, but they roughly cancel out [7].) And although the Bernoulli equation is intended for 'steady' (time-*in*dependent) flow [9], it can be used here assuming that the variation in fluid velocity is small ($\int_{s1}^{s2}\partial\mathbf{v}/\partial t \bullet d\mathbf{s}$~0) over the scales involved.

[17] Starting at the far end (node #20) and working backwards.

[18] Note:

When a streamline splits into parallel streams, the resulting Bernoulli expressions applied to each stream are all equal to each other: $P_A + \frac{1}{2}\rho v_A^2 = P_B + \frac{1}{2}\rho v_B^2 = P_C + \frac{1}{2}\rho v_C^2$
just as the voltages across parallel circuits are all equal to each other [10].

[19] From ALITRIG work, $v_{inj:0}$ is found to be ~50% higher than v_{jet}.

[20] The expression '$v_{inj:n}\{t_{n-1}\}$' should be read here as 'the injector speed along the n^{th} nodal section as the poison initially passes the $(n-1)^{th}$ node'. (Even when the poison has yet to reach the n^{th} node, there is still fluid flow along the entire injector, as there is unpoisoned D_2O originally throughout the injector [4].)

that contain each injector are horizontally spaced 8 lattice pitches apart and aligned such that two nozzle-streams are vertical. This arrangement was chosen to minimize poison-stream-overlap as the nozzle-streams expand, and maximize overall poison distribution.

When poison is injected through the assembly, it can either be directed wholly from one side to the other (*uni*-directional), or in a checkerboard pattern, with alternating injectors directing poison from one side or from the other (*bi*-directional). The former is the standard poison injection arrangement, while the latter is proposed as a method of reducing the likelihood of common-mode injection failure. That is, by having pressurized poison tanks on alternating sides of the core, the probability that an accident will affect both sides (disabling both sets of tanks) simultaneously is reduced. Both injection methods will be examined and compared here.

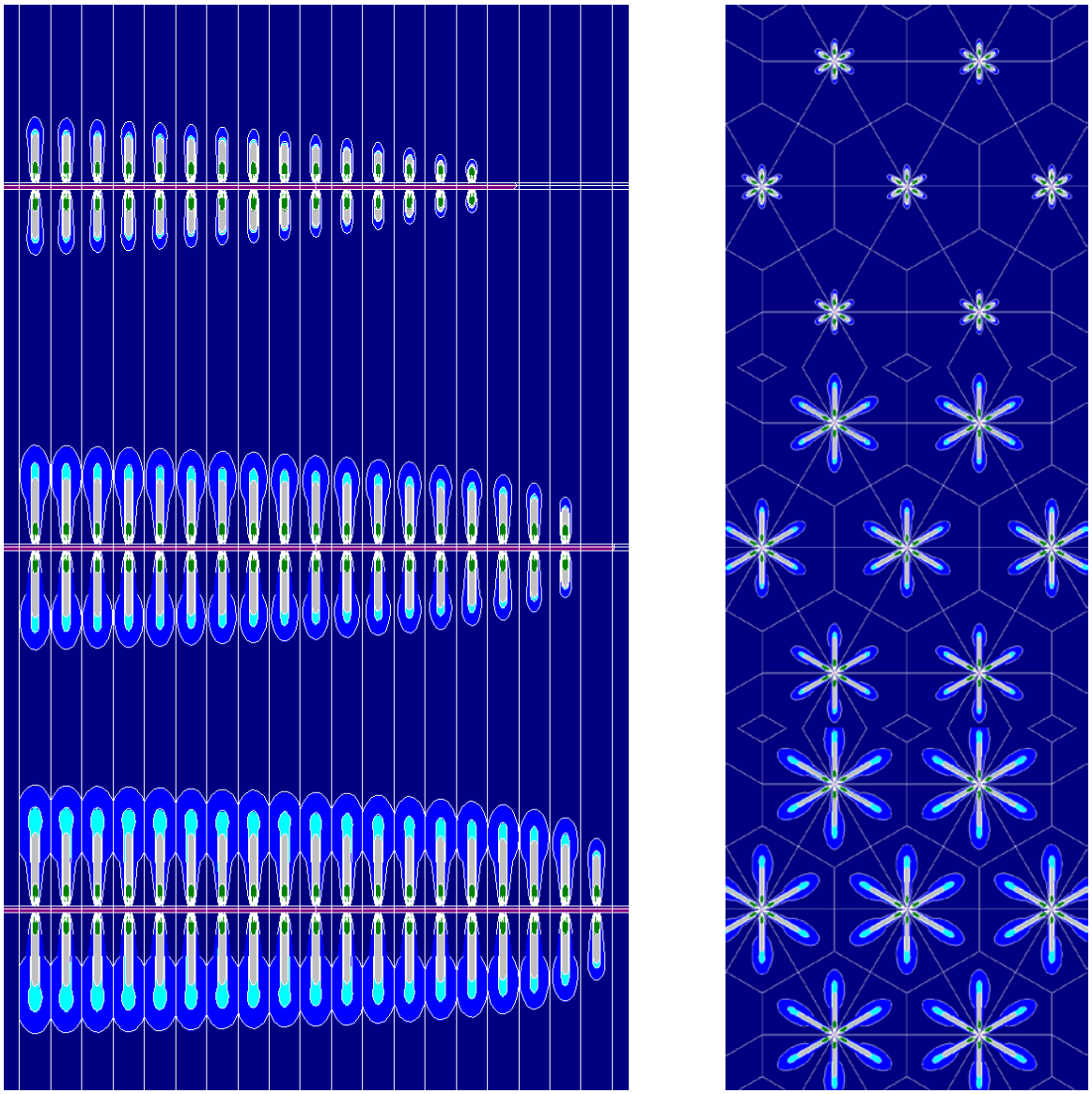

Figure 2-5 Modeled Poison Injection (Length-View & End-View @ ~0.2s, ~0.4s & ~0.6s)

3. Analysis & Results

The fuel assembly assumed here is based on that used in [1] (with the exception that the reactor model used here is not the infinite channel model used previously). The assembly has two rows of fuel elements around a central H_2O channel (used to suppress CVR and provide moderation for the inner row of fuel elements); see Figure 1-1. The MCNP model uses a simple cylindrical design for the fuel elements of the assemblies, ignoring details such as bundle endcaps\endplates.

Because the SCWR is a three-batch fuelled reactor, the fuel[21] modeled here is mixture of 'fresh' fuel, 'once-burned' fuel and 'twice-burned' fuel. The fuel consists of reactor-grade PuO_2 in a ThO_2 matrix, with the inner ring (nominally) at 15wt% PuO_2 and the outer ring (nominally) at 12wt% PuO_2 [13]. Here, fuel temperature was 687 K and D_2O purity was 99.833wt%.

To match the MCNP material-card temperatures, especially those for fuel & D_2O, with the various temperatures modeled for the SCWR, pairs of isotopic ratios at differing library temperature nodes (bracketing the actual temperature) were interpolated to the (square root of the) given temperature for each isotope[22]. Poison was modelled in the D_2O material cards based on the given Gd concentrations, with the rest of the D_2O isotopic concentrations renormalized. The density for D_2O was then adjusted according to given temperature and the amount of Gd.

In this analysis, MCNP6[23] [3] was run on the Titan cluster at CNL, using a cross-section library based on ENDF/B-VII.0 [14]. In all, 30 cases were here performed (15 uni-directional & 15 bi-directional) at 0.1 s intervals covering 0.0 s to ~1.4 s following poison injection into the core. Each case was run with 10,000 neutron histories per cycle and 1100 cycles (with the first 100 cycles dropped to ensure source convergence), for a total of 10 million histories per case. The reactivity results are shown in Figure 3-1, comparing both the uni- and bi-directional cases.

As can be seen, the reactivity drops off by ~100 mk in ~1 s (comparable to the reactivity drop in CANDU reactors; [15], [16]). Also, one can see that the reactivity drop for the bi-directional case (blue) is initially greater than that for the uni-directional case (red), but then the uni-directional case catches up to the bi-directional case by the end of the runs. This greater initial reactivity fall-off for the bi-directional case occurs because the poison is more spread out initially in the bi-directional case (as the poison is coming in from both sides) than in the uni-directional case. But by the mid-point, the poison in the uni-directional case starts to become well spread out also, and so the bi-directional case starts to lose its advantage over the uni-directional case. By the end of the runs, the poison is equally spread out, and their reactivity reductions are both equal.

---

21 Fuel burnup composition here determined by WIMS-AECL [11], [12].

22 So, given an assumed temperature T, and library temperature nodes T_{lo} & T_{hi} bracketing T, the 'lo' and 'hi' interpolation multipliers (multiplying each isotopic fraction) are given as:

$$f_{lo} = (T_{hi}^{½} - T^{½})/(T_{hi}^{½} - T_{lo}^{½}) \qquad f_{hi} = (T^{½} - T_{lo}^{½})/(T_{hi}^{½} - T_{lo}^{½})$$

where the interpolation is assumed linear in $T^{½}$ rather than T as neutron kinetic energy is proportional to $T^{½}$.

23 Used without the burnup option.

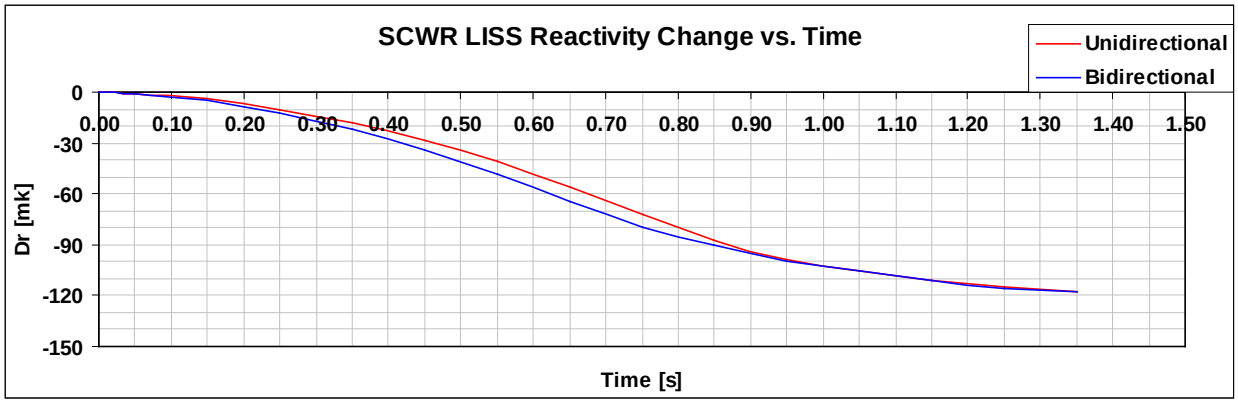

Figure 3-1 Reactivity Plot for Uni- & Bi-Directional Poison Injections

4. Summary

4.1 Discussion

In this analysis, an MCNP model for an SDS2 LISS was created and implemented for a finite SCWR reactor design from [1] and the resulting reactivity reduction studied. The reactivity was observed to drop off by ~100 mk in ~1 s (following poison injection into the core). The reactivity reduction achieved here compares favorably with the current poison injection systems in existing CANDU reactors; ~55 mk to ~95 mk in ~2 to 3 s [15], [16].

One concern for Th-reactors is that the delayed neutron fraction for U-233 is less than ½ that for U-235 [17]. In the SCWR, the majority of delayed neutrons will come from thermal fissions of isotopes of Pu-239, Pu-241 & U-233, which builds in from Th-232 during irradiation. The combined delayed neutron fractions from the isotopes of Pu and U-233 is ~½ of that from natural uranium fuel [18]. This effectively reduces the overall average neutron generation time by more than a factor of 2[24], which, in turn, reduces the response time for neutron transients by more than a factor of 2. Normally, this could pose issues with any emergency shutdown system if it fails to inject enough negative reactivity into the core during a shutdown. However, as can be seen above, the amount of negative reactivity injected into the core via the SDS2 is potentially twice that of CANDU for the same time interval. Thus, this modeled SDS2 system should then be more than adequate for the SCWR.

4.2 Conclusions

By utilizing previous studies on similar reactor designs (that is, the ACR), a poison injection system has been here modeled for the SCWR that achieves a sufficiently large reduction of reactivity (~100 mk) in a minimal amount of time (~1 s), thus lending credence to the viability of the SCWR concept.

4.3 Further Work

Since this analysis was done without any reactivity hold-down devices, further research with such devices present is needed. Additionally, further work should be done to determine how much of the saturation effect is due to the specific modeling used here, and, if possible, to verify these results via empirical studies. Also, the ‘reactivity worth’ of each of the 7 major isosyncs should be found to determine their individual contribution to reactivity reduction (for future poison-injection modelings). And, as the model used here allowed for bi-directional poison flow (proposed as a method of reducing the likelihood of common-mode injection failure), it might be of interest to further model LISS reactivity reduction assuming poison injection from one side or the other fails.

[24] The average neutron lifetimes are ~0.06s, ~0.03s & ~0.02s for U-235, U-233 & Pu-239, respectively [19].

5. References

[1] J. Pencer, D. Watts, A. Colton, X. Wang, L. Blomeley, V. Anghel and S. Yue, March 2013, "Core Neutronics for the Canadian SCWR Conceptual Design", Proc. of the 6th Int. Sym. SCWR (ISSCWR-6), Shenzhen, Guangdong, China.

[2] P.G.Boczar, W.Shen, J.Pencer, B.Hyland, P.S.W.Chan & R.G.Dworshak; "Reactor Physics Studies for a Pressure Tube Supercritical Water Reactor (PT-SCWR)"; *The 2nd Canada-China Joint Workshop on Supercritical Water-Cooled Reactors (CCSC-2010)*; Toronto, Ont., Canada; 2010 April 25-28.

[3] LANL; "MCNPX 2.6.0 Extensions", LA-UR-08-2216, http://mcnpx.lanl.gov; 2008, April 11.

[4] F.Song, R.Noghrehkar, K.F.Hau; "CFD Modelling of Liquid Poison Injection in ACR-1000 Shutdown System"; Proceedings of the 16th International Conference on Nuclear Engineering ICONE16, ICONE16-48669; May 11-15, 2008; Orlando, Florida, USA.

[5] H.Choi et al.; "Proliferation-Resistant Dry Process Oxide Fuel Technology Development"; KAERI\RR-2482\2004, http://www.iaea.org/inis/collection/NCLCollectionStore/_Public/37/077/37077659.pdf; Feb., 2005.

[6] http://en.wikipedia.org/wiki/Contour_line http://translate.google.com/?tl=el#en/el/concentration

http://www.greek-language.gr/greekLang/modern_greek/tools/lexica/triantafyllides/search.html?lq=συγκέντρωση

[7] K.M.Chae, H.Choi, B.W.Rhee; "Jet Flow Analysis of Liquid Poison Injection in a CANDU Reactor Using Source Term", KAERI\TR-1739\2001, http://www.iaea.org/inis/collection/NCLCollectionStore/_Public/32/062/32062422.pdf; Jan., 2001.

[8] Sect.3.2: http://www.engr.mun.ca/~yuri/Courses/MechanicalSystems/FlowAnalysis.pdf

[9] http://www.imc.pcz.czest.pl/instytut/pl/3/3.8/materialy/afm_bl/ube.pdf

[10] Sect.3.4.2: http://www.engr.mun.ca/~yuri/Courses/MechanicalSystems/FlowAnalysis.pdf

http://lofi.forum.physorg.com/bernoulli-equation-for-split-flow_14070.html

http://www.efm.leeds.ac.uk/CIVE/CIVE2400/pipe_flow2.pdf

[11] D.V.Altiparmakov; "New capabilities of the lattice code WIMS-AECL", *PHYSOR 2008: International Conference on Reactor Physics, Nuclear Power: A Sustainable Resource*; Casino-Kursaal Conference Center, Interlaken, Switzerland; 2008 Sept.14-19.

[12] WIMS-D Library Update, IAEA, 2007: http://www-nds.iaea.org/wimsd/libdata.htm

[13] M.Yetisir, M.Gaudet, D.Rhodes; "Development and Integration of Canadian SCWR Concept With Counter-Flow Fuel Assembly", 6th International Symposium on Supercritical Water-Cooled Reactors, ISSCWR-6; Shenzhen, Guangdong, China; Mar.3-7, 2013.

[14] D.V.Altiparmakov; "ENDF/B-VII.0 Versus ENDF/B-VI.8 in CANDU Calculations", *PHYSOR 2010: Advances in Reactor Physics to Power the Nuclear Renaissance*; Pittsburgh, Penn., USA; 2010 May 9-14.

[15] https://canteach.candu.org/Content%20Library/20050615.pdf, Table 3.

[16] https://canteach.candu.org/Content%20Library/20041113.pdf, Table-13-3.

[17] https://www.gen-4.org/gif/upload/docs/application/pdf/2013-10/gif_egthoriumpaperfinal.pdf

[18] J.Pencer, M.McDonald, and V.Anghel, "Parameters for Transient Response Modeling for the Canadian SCWR", The 19th Pacific Basin Nuclear Conference (PBNC 2014), Vancouver, B.C., Canada; 2014 Aug24-28.

[19] J.J.Duderstadt, L.J.Hamilton; "Nuclear Reactor Analysis"; John Wiley & Sons, Dept.of Nuclear Engineering, Univ. of Michigan, Ann Arbor, Michigan; 1976.